Surface shift of the occupied and unoccupied 4f levels of the rare-earth metals

Aldén, Magnus; Johansson, Börje; Skriver, Hans Lomholt

Published in:
Physical Review B

Link to article, DOI:
10.1103/PhysRevB.51.5386

Publication date:
1995

Document Version
Publisher's PDF, also known as Version of record

PHYSICAL REVIEW B VOLUME 51, NUMBER 8 15 FEBRUARY 1995-II

Surface shift of the occupied and unoccupied $4f$ levels of the rare-earth metals

M. Aldén* and B. Johansson
Condensed Matter Theory Group, Physics Department, Uppsala University, S-75121 Uppsala, Sweden

H. L. Skriver
Center for Atomic-Scale Materials Physics and Physics Department, Technical University of Denmark, DK-2800 Lyngby, Denmark

(Received 6 September 1994)

The surface energy shifts of the occupied and unoccupied $4f$ levels for the lanthanide metals have been calculated from first principles by means of a Green's-function technique within the tight-binding linear muffin-tin orbitals method. We use the concept of complete screening to identify the occupied and unoccupied $4f$ energy level shifts as the surface segregation energy of a $4f^{n-1}$ and $4f^{n+1}$ impurity atom, respectively, in a $4f^n$ host metal. The calculations include both initial- and final-state effects and give values that are considerably lower than those measured on polycrystalline samples as well as those found in previous initial-state model calculations. The present theory agrees well with very recent high-resolution, single-crystal film measurements for Gd, Tb, Dy, Ho, Er, Tm, and Lu. We furthermore utilize the unique possibility offered by the lanthanide metals to clarify the roles played by the initial and the different final states of the core-excitation process, permitted by the fact that the so-called initial-state effect is identical upon $4f$ removal and $4f$ addition. Surface energy and work function calculations are also reported.

I. INTRODUCTION

The first observation of a surface core-level shift (SCLS) was made for a lanthanide metal, samarium, where a shift of about 7 eV for the $3d$ level was found in the x-ray photoelectron spectroscopy spectrum.[1] However, at first it was not recognized as a SCLS and was instead interpreted as a sign of mixed valence behavior in the bulk metal. This interpretation was refuted in Ref. 2 and it was suggested that the observed divalent signal originated from a surface induced effect. Later it was quite clearly demonstrated experimentally that samarium metal, which in the bulk is a trivalent lanthanide metal, at the surface had turned into a divalent configuration.[3,4] Theoretical considerations gave complete support to this view.[5] A number of years later, it was shown that for relatively badly prepared thulium surfaces one could observe a divalent signal at the surface[6] in contrast to the trivalent bulk, this also in accordance with theory.[5,7,8]

In the case of samarium the presence of a surface apparently gives rise to particularly strong effects, so that the valence configuration changes from $4f^5$ (bulk) to $4f^6$ (surface). This in turn leads to a very pronounced redistribution of the atomic charge density, which explains the extraordinarily large 7 eV shift of the $3d$ level.[9,10] Later, one observed surface shifts of the $4f$ level between surface and bulk atoms also for metals where there was no change in valence. Theory, where a complete screening of the final state was assumed and which was combined with a simple estimate of surface energies, predicted a shift of about 0.4 eV for the trivalent lanthanides and 0.5 eV for the divalent metals.[5] In a thorough experimental investigation by several workers,[8,11] it was found that the SCLS varied from 0.4 eV to about 0.7–0.9 eV when proceeding through the series from La to Lu.

In connection with the study of rare-earth surface magnetism, there has been a renewed interest in the surface $4f$ energy-level shifts of the lanthanides.[12–17] As a result, for several metals there are now single-crystal data available.[13–16] On the theoretical side, it has become possible to study the surface core-level shifts by means of *ab initio* calculations,[18–22] where both initial- and final-state effects are taken into account within the concept of complete screening.[9,10,23–26] Therefore, it is of interest to make a comparison between theory and experiment for this class of elemental metals, where the effect of small changes in the electronic structure can be monitored as one proceeds from one element to the next in the series.

In this paper, we present a theoretical study of the surface $4f$ binding energy shifts ($4f$ removal shift) and the surface shift of the unoccupied $4f$ levels ($4f$ addition shift) for close-packed surfaces of the lanthanide metals. We use a Green's-function technique based on the tight-binding linear muffin-tin orbitals method, and within the assumption of complete screening we identify the $4f$ removal and $4f$ addition shifts with the surface segregation energy of a correspondingly $4f$ excited atom. Therefore, our calculations include the so-called final-state effects which, as demonstrated by the latest experimental findings,[13–17] are important for the rare-earth metals. We do not, however, take into account the possible magnetic effects which may arise due to the presence of an open $4f$ shell and instead include the $4f$ levels in a frozen, paramagnetic core, obtained in a fully relativistic treatment.

0163-1829/95/51(8)/5386(11)/$06.00

II. COMPUTATION

A. The Green's-function techniques

The present calculations are based on local-density theory[27] and the scalar-relativistic tight-binding linear muffin-tin orbitals method (TB-LMTO). We use a minimal (*spd*) basis set and the second-order expressions for the Hamiltonian, potential functions, and partial waves.[28,29] In addition, we apply the frozen-core approximation and the atomic sphere approximation (ASA) for the intrasphere potential but include both monopole and dipole contributions to the electrostatic intersphere potentials.[30] In the surface calculations we employ the Green's-function technique, which accounts properly for the breakdown of translational symmetry which occurs at a surface, as implemented within the TB-LMTO formalism by Skriver and Rosengaard.[30,31] To generate the surface Green's-function matrices, we utilize the efficient principal-layer technique.[32–34] This Green's-function method has been used in studies of surface energies and work functions,[31,35] surface and interface magnetism,[36,37] and stacking fault energies[38] of elemental metals.

The present $4f$ energy-level shift calculations are based on the complete screening picture, i.e., the assumption that the symmetrical part of the measured $4f$ line profile corresponds to a completely screened state in which the conduction electrons have attained a fully relaxed configuration in the presence of a hole in the $4f^n$ shell.[23] Following Herbst *et al.*[9,10] and Johansson,[24] we apply the analogous screening assumption also for the $4f$ addition shifts. This framework requires total-energy computations of a substitutional impurity located in the bulk or at the surface, and the surface shift of the $4f$ binding energy may be identified with the surface segregation energy of a $4f^{n-1}$ impurity.[26] For the $4f$ addition energy level, the surface shift may be identified with the surface segregation energy of a $4f^{n+1}$ impurity atom. Since most of the lanthanides are trivalent metals, the $4f^{n-1}$ energy shift corresponds to a surface segregation energy of a tetravalent impurity. Accordingly, the $4f^{n+1}$ surface shift corresponds in most cases to a divalent impurity atom segregating to the surface.

The Green's-function technique has recently been extended[20–22] to allow bulk and surface impurity calculations and has been used in investigations of surface core-level shifts for a wide range of transition and simple metals.[20–22,39] In these calculations, the cluster Green's functions for the bulk and the surface impurities are constructed in a completely analogous manner to reduce numerical sources of errors[22] and under the proper bulk or surface boundary conditions, i.e., we do not use a slab geometry. In the study of the lanthanide metals we treat the open $4f$ shell as a part of the (paramagnetic) frozen core, whereby effects due to, e.g., magnetism are not accounted for. In the removal process, the neutral $4f$-ionized impurity is a host atom where one $4f$ electron is replaced by one extra valence electron while in the $4f$ addition process, the impurity is formed by transferring on one host atom one valence electron into the $4f$ shell.

B. The total energy

Within the Born-Oppenheimer and local-density approximations, the total energy is a functional of the charge density and may, within the ASA and frozen-core approximations, be evaluated essentially from the spherically averaged charge density inside overlapping, space-filling spheres. However, in the summation of the electrostatic intersphere contributions the inclusion of both monopole-monopole and monopole-dipole interactions was found[30] to be a necessary step beyond the ASA for surface calculations by the present technique. The method provides a consistent and accurate description of the surface energy for close-packed surfaces[30,31] where the discrepancy between theory and the crystal-structure independent data of de Boer *et al.*[40] is usually less than 10–15 %. Notable exceptions are, however, the first elements in the d transition metal series, where the surface energy may be underestimated by up to 50% in comparison[31] with both experiment[40] and independent so-called full-potential calculations.[41] For the lanthanide metals, which are at focus in the present work, a similar discrepancy is expected since the lanthanides may all be regarded as early $5d$ transition metals as far as the valence electron properties are concerned.

In order to improve the credibility of the calculated surface core-level shifts, which indirectly rely on how well the surface energies are represented, it is desirable to consider improvements to the ASA total-energy functional. Recently, Kollár and co-workers[42,43] studied this problem in connection with surface energy calculations for the light actinide metals. They concluded that one may obtain accurate surface energies also for the early transition elements and actinides provided one calculated the electrostatic Coulomb contribution to the total energy (a) from the full, nonspherical charge density, constructed within a one-center expansion from the output of the ASA surface calculation, and (b) performed the space integrals over the correct Wigner-Seitz cell rather than over overlapping atomic spheres.[42] Here, we shall only apply the first and most important of these two corrections which amounts to evaluating the total energy by means of the full valence charge density within overlapping, space-filling spheres and to perform a complete summation of the intersphere electrostatic terms. This is the spherical cell model (SCM) of Ref. 42. As we shall see, the SCM functional improves the agreement with experiment for the surface energy, and for the calculated SCLS the difference between ASA and SCM is appreciable for the divalent metals but less significant for the trivalent metals. It should be noted that the SCM functional works so well because both the kinetic energy and the total energy obey a variational principle.

Within the ASA and SCM functionals, the total energy including the electrostatic contributions is conveniently partitioned into atomic-sphere dependent terms. The surface energy is thereby calculated as the sum[30,31]

$$E_S = \sum_Q^S (E_Q^{2D} - E_Q^{3D}), \tag{1}$$

over the surface region S of the differences between the total energy E_Q^{2D} projected onto site Q and the corresponding energy E_Q^{3D} obtained in the underlying bulk calculation.

The surface segregation energy is defined as the energy required to interchange an impurity atom in the bulk with a host atom at a particular surface site Q_S. For a complete separation of the bulk and surface impurity problems, employing the formalism detailed in Ref. 22, the segregation energy may be obtained from

$$E_{\rm segr}^{\rm imp} = E_{\rm surf}^{\rm sol} - E_{\rm bulk}^{\rm sol} - E_{S,Q_s}, \qquad (2)$$

in terms of the solution energies of the impurity located in the bulk ($E_{\rm bulk}^{\rm sol}$) and at the surface ($E_{\rm surf}^{\rm sol}$), respectively, minus the Q_s projected surface energy E_{S,Q_s} of a host atom. The last term accounts in the ASA for the exchange of a host atom at the surface impurity site with an impurity atom at a bulk site, as required in the segregation process. For the present application of Eq. (2) to the case of a neutral $4f^{n\mp1}$ impurity in the $4f^n$ metal host, a positive $4f$ level shift corresponds to a higher binding energy for the surface $4f$ state than for the bulk $4f$ state in the case of $4f$ removal, and in the case of $4f$ addition a positive shift corresponds to a higher energy position above the Fermi level for the surface $4f$ state than for the bulk $4f$ state.

C. Details of the calculations

In the surface calculations, we allow relaxation of the charge density and potential in six layers below the surface plane together with two layers simulating the vacuum. For the bulk and surface impurity calculations, we use a cluster region consisting of the impurity site plus eight shells of neighbors for the hcp lattice and four shells for the bcc and fcc lattices, corresponding to a total of 51, 51, and 55 atoms, respectively, in the cluster. For the summation of the one-electron contribution to the impurity solution energies we utilize the generalized phase shift as suggested by Gunnarsson *et al.*,[44] whereby the solution energies are estimated to be converged in shell number to within ± 0.02 eV. The Green's functions are sampled on 16 energy points spaced exponentially on a semicircle in the complex energy plane. In the underlying bulk calculations we use 1785 k points in the irreducible wedge of the Brillouin zone for the bcc structure, 1505 points for the fcc structure, and 1500 points for the hcp structure. In the surface k-space integration, we use 252 special $k_{\|}$ points in the irreducible part of the two-dimensional Brillouin zone for the hcp(0001) and fcc(111) surfaces, 256 points for the bcc(110) surface, and 136 points for the fcc(100) surface.

III. RESULTS

In the following we shall present calculations of the surface energy, work function, and surface energy shifts for the occupied (removal) and unoccupied (addition) $4f$ states of the rare-earth metals. For the surface energy and work function the calculations are based on the Green's-function technique for the clean surface, the self-consistent solution of which provides the input to the following surface impurity calculation, which, as mentioned above, is completely separated from the bulk impurity Green's-function calculation. We use the most close-packed surface of the experimentally observed crystal structures at the experimentally determined atomic volumes, except for samarium and the dhcp elements which are treated as hcp. The crystal structures we have used are as follows: Ba(bcc), La (hcp), Ce (fcc), Pr (hcp), Nd (hcp), Pm (hcp), Sm(hcp), Eu(bcc), Gd(hcp), Tb (hcp), Dy (hcp), Ho (hcp), Er (hcp), Tm (hcp), Yb (fcc), and Lu (hcp). In addition, for a restricted set of elements the $4f$ energy shift calculations are performed for several crystal structures. We neglect relaxation of the surface layer positions and do not consider the abnormal valency change at the Sm surface, owing to the complexity of the corresponding *ab initio* calculation. Hence, Sm is treated on the same footing as the other trivalent metals. This also applies to Ce, which is calculated for an atomic volume appropriate for the γ phase.

A. Surface energy

The experimentally deduced surface energies of the lanthanide metals, obtained within the framework of the macroscopic-atom model by de Boer *et al.*,[40] are reproduced in Fig. 1 and they exhibit a slow, linear increase as one proceeds through the trivalent rare-earth elements

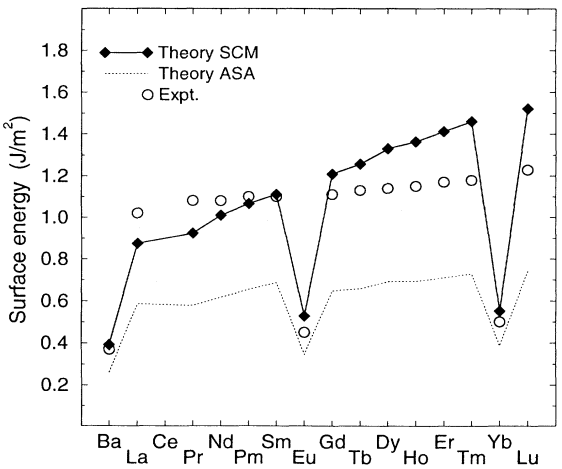

FIG. 1. The calculated surface energy for the most close-packed surface of either the hcp, fcc, or bcc crystal structure of the rare-earth metals (see text). Solid symbols refer to calculations using the SCM energy functional, and the ASA results (dotted line) are included for comparison. All elements have been treated as trivalent, except Ba, Eu, and Yb, which are divalent. The surface-independent experimental data are marked with open circles.

from La to Lu. This may seem surprising on the basis of the fact that the d-electron occupancy is continuously reduced from about 2.0 in La to 1.4 in Lu,[45,46] whereby according to the simple picture of d-electron contribution to the cohesive and surface energies[47] La should have a higher surface energy than Lu. The behavior in the lanthanide series is, however, more appropriately explained as a result of the reduction in atomic volume with increasing atomic number, usually referred to as the "lanthanide contraction."[48] The volume contraction leads to an increase of approximately 20% in the surface charge transfer when proceeding from La to Lu and from this follows the observed increase in the surface energy.

In Fig. 1, we compare the ASA and SCM surface energy results with the crystal structure independent experimental values of de Boer *et al.*[40] In this comparison, it is seen that for the trivalent metals the ASA functional underestimates the surface energy by a factor of ≈ 2 in comparison with the de Boer data. In contrast, the results of the SCM functional are in much better agreement with experiment, although when regarding the trend across the series the SCM seems to give too large an increase in the surface energy which, on the other hand, the ASA reproduces remarkably well. For the divalent metals Ba, Eu, and Yb, both experiment and theory in Fig. 1 suggest surface energies at an essentially constant level across the series. For these elements, also, the differences between the ASA and SCM results are smaller than what is found in the case of the trivalent metals.

The surface shift of the 4f-addition state for a trivalent lanthanide metal may approximately be obtained from the difference in surface energy between the (hypothetical) divalent ($4f^{n+1}$) and trivalent ($4f^{n}$) elements rather than from the difference between the surface energy of the $(Z+1)$ and Z metals.[26] Therefore, a proper account of the separation between the divalent and trivalent surface energy curves seems to be of greater relevance for the SCLS than the slope of the surface energy curve as one proceeds from the left to the right in the series. Moreover, we find that the SCLS is less sensitive to the actual total-energy functional than the surface energy due to the fact that the SCLS is essentially a second-order difference in total energies and therefore seems to benefit more than the surface energy from a cancellation of errors.

B. Work function

To our knowledge there are no single-crystal work function measurements available for any of the lanthanide metals, and we, therefore, compare in Fig. 2 and Table I our calculated work functions with the limited amount of polycrystalline data compiled for the rare earths by Michaelson.[49] We notice that the theoretical work functions show a slow rise for both the divalent and trivalent elements as one moves across the series. This is mainly caused by a corresponding increase in the charge transfer and hence the dipole barrier at the surface. For the lower density divalent metals, the calculations suggest a lowering of the work function by approximately 1 eV as compared to the more dense trivalent metals. This seems to be consistent with the comparatively small work functions observed for divalent Ba and Eu.

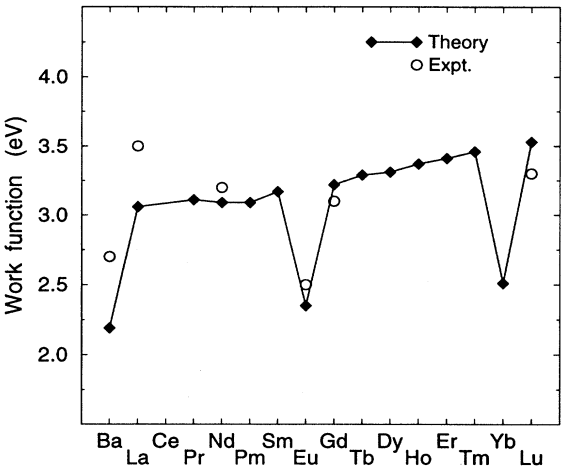

FIG. 2. Comparison between the experimental work function for polycrystalline samples (open circles) and the calculated work function (squares) for the most close-packed surface of either the hcp, fcc, or bcc crystal structures of the rare-earth metals (see text). All elements in the calculations have been treated as trivalent, except Ba, Eu, and Yb, which are divalent.

C. Surface 4f removal shift

The shift in binding energy between a surface and a bulk atom upon removal of a corelike 4f electron has been studied extensively for the lanthanide metals dur-

TABLE I. Work functions and surface energies for the lanthanide metals. The experimental work functions in parentheses are polycrystalline values.

Metal	Surface	Work function		Surface energy		
		Theory	Expt.[a]	Theory		Expt.[b]
		(eV)	(eV)	(eV)	(J/m^2)	(J/m^2)
Ba	bcc(110)	2.19	(2.7)	0.391	0.432	0.37
La	hcp(0001)	3.06	(3.5)	0.670	0.875	1.02
Ce	fcc(111)	3.26		0.619	0.862	
Pr	hcp(0001)	3.11		0.673	0.924	1.08
Nd	hcp(0001)	3.09	(3.2)	0.723	1.010	1.08
Pm	hcp(0001)	3.09		0.755	1.065	1.10
Sm	hcp(0001)	3.17		0.781	1.111	
Eu	bcc(110)	2.35	(2.5)	0.487	0.526	0.450
Gd	hcp(0001)	3.22	(3.1)	0.864	1.209	1.11
Tb	hcp(0001)	3.29		0.880	1.256	1.13
Dy	hcp(0001)	3.31		0.928	1.331	1.14
Ho	hcp(0001)	3.37		0.943	1.364	1.15
Er	hcp(0001)	3.41		0.967	1.413	1.17
Tm	hcp(0001)	3.46		0.990	1.462	<1.18
Yb	fcc(111)	2.51		0.448	0.551	0.50
Lu	hcp(0001)	3.53	(3.3)	1.011	1.523	1.23

[a]See Ref. 49.
[b]See Ref. 40.

ing the past one and a half decade. The pioneering work on Sm,[3] where a valence change at the surface gives rise to an extraordinary −7.6 eV binding energy shift of the $3d$ level, was followed by numerous measurements on the other lanthanide metals, and a useful compilation of these SCLS recordings is for instance given by Flodström *et al.*[8] In this compilation one finds surface $4f$ binding energy shift data in the range from approximately 0.4 eV to 0.8 eV, increasing with increasing atomic number. These experiments, obtained solely from polycrystalline surfaces, were found to agree remarkably well with calculated initial-state (core-eigenvalue) shifts by Begley *et al.*,[50] using a LMTO slab representation of the hcp(0001) surface.

In a recent series of high-resolution experiments on the single-crystal hcp(0001) surface of Gd (Ref. 14) and Tb (Ref. 13) Kaindl and co-workers have reported a reduction in the measured surface shift by approximately a factor of 2 as compared to the older data.[8] This suggests that the previous agreement between the computed initial-state shifts[50] and polycrystalline measurements was somewhat fortuitous, and that the so-called final-state effects need to be included in a theoretical treatment of the surface $4f$ shifts for the lanthanide metals, which thus motivates the present work.

The calculated $4f$ surface binding energy shift for the most close-packed facet of the experimentally observed crystal structures, approximating the dhcp and Sm structure by hcp, are presented in Fig. 3 together with the available experimental data. Again, we make a comparison between the results obtained using the ASA and SCM functionals for the total energy description, respectively, and find that the difference between these two separate sets of results for the SCLS is rather small. The largest discrepancy between ASA (dotted line) and SCM (solid squares) is found for the divalent metals Ba, Eu, and Yb, where it is of the order 0.1 eV, and where we have used the bcc(110), bcc(110), and fcc(111) facets, respectively, for this comparison. In what follows, we shall only refer to the SCM results, i.e., those which are tabulated in Tables I and II and which thus form the recommended theory.

For the trivalent metals in the lower panel of Fig. 3, it is seen that both the older polycrystalline measurements (circles) of the surface $4f$ binding energy shift and the theoretical values (solid squares) exhibit a characteristic gradual increase across the series. Hence, according to the polycrystalline data the variation of the surface shift across the series is well described by the present theory. On the other hand, it is also clear from Fig. 3 that the present type of calculations gives surface shifts which are significantly lower than both the earlier measurements on polycrystalline samples[8] and the aforementioned previous computations[50] based solely on the initial-state model.

The recordings for single-crystal Tb(0001) (Ref. 13) and Gd(0001) (Ref. 14) surfaces significantly reduce this discrepancy between the present theory and experiment. The surfaces of Tb and Gd were created by means of thermal evaporation and layer-by-layer monocrystalline growth on a W(110) substrate,[13,14] and the film was found to be magnetic for Gd and nonmagnetic for Tb.[17] In these elements the measured SCLS are even slightly lower than our calculated shifts. Rather surprisingly, the experimental values decrease from Gd to Tb, in contrast to the general behavior across the series. However, when proceeding from Tb towards the heavier lanthanides the most recent experimental findings[15] again follow the increasing trend, and for the sequence Dy-Lu, the agreement between experiment and theory is almost perfect.

It thus remains to be understood what causes the relatively irregular behavior in the single-crystal measurements in the sequence Gd-Er. In particular, the anomalously small measured shift for Tb is difficult to understand, especially in view of the good agreement between theory and experiment obtained for the sequence Dy-Ho. We may, for instance, speculate that the surface reso-

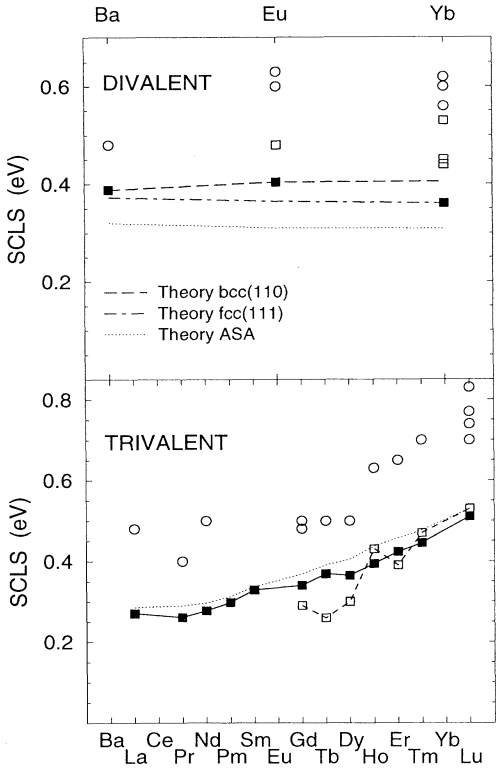

FIG. 3. The calculated surface shift (solid squares) of the occupied $4f$ states [note Ba($4d$) and La($4p$)] for the most close-packed surface of either the hcp, fcc, or bcc crystal structures of the rare-earth metals (see text). The results for the divalent metals (bcc Ba, bcc Eu, and fcc Yb), and the trivalent (hcp) metals are presented separately in the top and bottom panels, respectively. Comparison is made between calculations using the SCM (solid squares) and the ASA (dotted line) energy functionals. In addition, for the divalent metals a consistent comparison is made between separate series of calculations for the bcc(110) (long-dashed) and the fcc(111) (dot-dashed) surfaces. Experimental polycrystalline and single-crystal data are marked with open circles and open squares, respectively, with references given in Table II.

nance which appears close to the Fermi level[51] only in the high quality samples,[13,14,17] and which is also seen in calculations elsewhere,[22] does itself increase the sensitivity to a nonperfect surface termination. In a previous calculation[22] for trivalent Lu an unexpected lowering of the SCLS was obtained when proceeding from hcp(0001) to the less close-packed (hypothetical) fcc(100) facet.[52] On the other hand, it has been conjectured that the position of the 5d resonance is erroneously reproduced by LDA surface calculations.[17] Finally, one should again be aware of some of the approximations used in the present calculations, such as the neglect of magnetic effects in conjunction with the frozen-core approximation, and the omission of surface layer relaxations.

For the divalent sequence Ba-Eu-Yb in the top panel of Fig. 3, the computed shifts remain practically constant through the series. This is especially true when the crystal dependence is removed and the calculations are performed for the same crystal and surface for all three divalent elements, as demonstrated by the almost flat and parallel curves for the bcc(110) (dashed) and the fcc(111) (dot-dashed) facets in Fig. 3. For these elements, when proceeding from Ba to Yb, there is a reduction in the atomic volume of approximately 21 Å^3 (34%), which should be compared to the 7.8 Å^3 (21%) reduction occurring in the trivalent sequence between La and Lu. However, the considerably higher electron density experienced by the trivalent metals as compared to the divalent metals makes the effect of the volume reduction on, e.g., the surface potential and the cohesive properties, much more pronounced in the trivalent set, and this, we argue, explains the different sequential behavior in the divalent and trivalent series of elements in the top and bottom panels, respectively, of Fig. 3.

In the experimental polycrystalline data for the divalent metals in the top panel of Fig. 3, the theoretical

TABLE II. Surface core-level removal shift (left) and 4f-addition shift (right) of the lanthanide metals. In the removal case, the core level in question is the occupied 4f level, except for Ba (4d) and La (4p or 5p). The experimental shifts in parentheses are polycrystalline values.

Metal	Surface	Core-level shift (eV)		4f-addition shift (eV)	
		Theory	Expt.[a]	Theory	Expt.
Ba	bcc(110)	0.388	(0.48)[b]		
	fcc(111)	0.373			
La	hcp(0001)	0.271	(0.48)	-0.424	(−0.65)[c], −0.64[d]
	fcc(111)	0.337		-0.563	
Ce	fcc(111)	0.304		-0.428	
	hcp(0001)	0.248		-0.389	
Pr	hcp(0001)	0.261	(0.4)	-0.438	
Nd	hcp(0001)	0.278	(0.5)	-0.441	
Pm	hcp(0001)	0.298		-0.477	
Sm	hcp(0001)	0.329		-0.465	
Eu	bcc(110)	0.404	(0.60),0.48[e]	-0.638	
	hcp(0001)	0.315			
	fcc(111)	0.365			
Gd	hcp(0001)	0.340	(0.48),0.29[f]	-0.542	-0.48[c]
Tb	hcp(0001)	0.369	(0.50),0.26[g]	-0.571	
Dy	hcp(0001)	0.365	(0.50),0.30[h]	-0.606	
Ho	hcp(0001)	0.394	(0.63),0.43[h]	-0.626	
Er	hcp(0001)	0.423	(0.65),0.39[h]	-0.641	
Tm	hcp(0001)	0.445	(0.70),0.47[h]	-0.660	
Yb	fcc(111)	0.361	(0.56–0.62),0.53[i], 0.44[j], 0.45[h]		
	fcc(100)	0.461			
	bcc(110)	0.405			
Lu	hcp(0001)	0.511	(0.70–0.83),0.53[h]		
	fcc(100)	0.468			

[a]Flodström *et al.* (Ref. 8) and references therein.
[b]Jacobi *et al.* (Ref. 53).
[c]Fedorov *et al.* (Ref. 12).
[d]Fedorov *et al.* (Ref. 16).
[e]E. Weschke, C. Laubschat, and G. Kaindl (private communication).
[f]Fedorov *et al.* (Ref. 14).
[g]Navas *et al.* (Ref. 13).
[h]Kaindl *et al.* (Ref. 15).
[i]Mårtensson *et al.* (Ref. 59).
[j]Stenborg *et al.* (Ref. 60).

picture of a constant shift across the Ba-Eu-Yb sequence is not as clearly seen. For bcc Ba, however, only a single measured value has been reported,[53] whereas in the rich data set for fcc Yb the values are scattered considerably. This is also the case for the three lowermost Yb(111) results (open squares) which are referred to as "single crystal" in the experimental literature.[8,17,15] Hence, uncertainties in the experimental data set appear to be difficult to rule out, which is also reflected in the irregularity of the measured shifts for the trivalent metals when proceeding from one element to the next.

D. Surface $4f$ addition shift

The energy position of the unoccupied $4f$ levels relative to the Fermi level for the lanthanide metals was first studied by Lang *et al.*[54] using bremsstrahlung isochromat spectroscopy (BIS). For the theoretical interpretation of the unoccupied $4f$ level, Herbst *et al.*[9,10] and Johansson[24] applied the complete screening picture in which an electron is taken from the Fermi level and placed into the f shell of a specified ion. In this case the complete screening assumption means that the excited $4f$ addition state, corresponding to the BIS signal, is *localized* and completely screened by the conduction electrons, so that the metallic site is essentially converted into an impurity with a *lower* integral valence state than the host metal. By considering the free atomic excitations and regular values of the cohesive energy of the divalent and trivalent metals, and to a first approximation disregarding the impurity aspect, the measured bulk energy positions of the unoccupied $4f$ states could be reproduced very well.[24]

A bulk to surface shift for the unoccupied $4f$ levels have recently been measured by means of inverse photoemission for polycrystalline La (Ref. 12) and single-crystal Gd(0001) (Ref. 14). The observed -0.65 eV shift for polycrystalline La was found to be consistent with semiempirical estimates of the surface segregation energy of a divalent impurity atom, i.e., applying the complete screening picture, and taking into account the roughness of the polycrystalline surface in an approximate way.[12] For the case of the *single-crystal* dhcp La(0001) surface, the first experimental analysis suggested a $4f$ addition shift of the order -0.34 eV,[17] but today the La(0001) value is experimentally resolved at -0.64 eV.[16] This is remarkably similar to the previous polycrystalline result,[12] but disagrees strongly with the present type of calculations (see below), as is evident in Fig. 4. In single-crystal Gd(0001), however, the measured unoccupied shift was found to be -0.48 eV, while the shift of the occupied $4f$ level was $+0.29$ eV. These single-crystal findings for Gd(0001) (Table II) suggest that the magnitude of the $4f$-level shifts is significantly larger for the unoccupied state than for the occupied state.

In Fig. 4, we present calculations of the surface $4f$ addition shift for the most close-packed surface of the lanthanide metals, in the form of the surface segregation energy of a $4f$-addition state impurity. The calculational method is completely analogous to the one used above for the $4f$-removal SCLS, except that here the impurity is prepared with an opposite change of the occupancy in the valence and $4f$ shell, respectively. Among the divalent lanthanides only bcc Eu has been included, since for Ba the unoccupied $4f$ orbital is probably too extended to be regarded as a genuine core level,[24] which, as a result, makes the Ba $4f$ orbital difficult to converge within a conventional one-electron core calculation. For the trivalent metals, however, it is seen in Fig. 4 that also the shift of the unoccupied $4f$ level is predicted to exhibit a characteristic increase in magnitude through the series, from -0.42 eV for La to -0.66 eV for Tm, which is the last element in the series for which a $4f$ level is unoccupied. There is thus an astonishing similarity in the behavior of the $4f$ removal and $4f$ addition shifts, except that the $4f$ addition shifts are negative with the sign convention used by Eq. (2) and, for the case of the trivalent metals, their magnitude is approximately 50% larger than for the removal shifts. In anology with the $4f$ removal case the theory seems to slightly overestimate the magnitude of the BIS result for Gd(0001).[14] As regards the surface $4f$ addition shift in La, the severe deviation between theory and experiment in Fig. 4 is unexpected. Assuming that the experimental data are correct, one has to consider possible erroneous assumptions in the theoretical approach. Since the deviation occurs for the first element in the series one might question to what extent the localized (nonbonding) picture of the unoccupied $4f^1$ La orbital is valid. The absolute value of the $4f^1$ La addition energy shows a much less satisfactory agreement with theory[24] than does the corresponding $4f$ addition energy for all the other lanthanide metals, possibly suggesting a less well-defined localized $4f^1$ state for lanthanum.

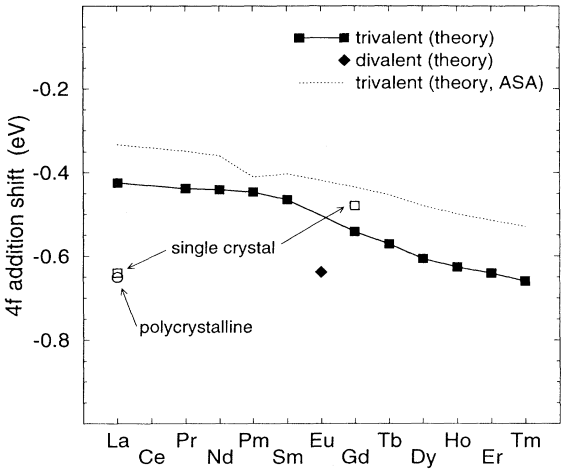

FIG. 4. The calculated surface shift of the unoccupied $4f$ states for the most close-packed surface of the bcc or hcp crystal structures of the divalent and trivalent, respectively, rare-earth metals. The result for divalent bcc Eu is marked separately with a solid diamond. For the trivalent metals comparison is made between calculations using the SCM (solid squares) and ASA (dotted line) energy functionals. Experimental polycrystalline and single-crystal data are marked with open circles and open squares, respectively, with references given in Table II.

IV. INITIAL- AND FINAL-STATE EFFECTS

Within the complete screening picture the surface shift of the occupied or unoccupied $4f$ energy levels is obtained as a total-energy difference between the two different *final states* of the surface and the bulk $4f$ electron excitation process, respectively. In this interpretation of the binding energy shift there is no explicit connection to the initial state of the removal-addition ionization processes, except for the fact that the final state is a product of the initial state.[55] The situation in the lanthanide series is particularly interesting because we can monitor two opposite final states, namely, shifts of the $4f$ removal and the $4f$ addition energies.[14] For normal metals, such a situation never occurs and one can only consider shifts of the ionization energy for a core level. Since for the $4f$ metals the initial state is the same for both the removal and the addition excitation processes, it follows that within the initial-state picture the surface shifts of the two excitation processes, apart from a change of sign, should be identical. Thus the mere observation of a different surface shift for the $4f^{n-1}$ and $4f^{n+1}$ levels demonstrates the limitation of the initial-state picture.[14,56]

Before we discuss the initial-state model in terms of the shift of the valence-band centroid, we present in Fig. 5 the calculated $5d$ valence-state occupancy as a function of atomic number. In the left-hand panel, we show the initial-state $5d$ bulk occupancies for the divalent and trivalent metals which exhibit the well-known (theoretical) reduction of the d occupancy with increasing atomic number. In the left-hand panel we show the $5d$ contribution to the screening charge, defined as the difference in $5d$ occupancy, after and before core excitation, projected onto the impurity atomic sphere. It is seen that for the trivalent metals the screening charge upon $4f$ removal consists of almost exactly one d electron, whereas the screening charge upon $4f$ addition corresponds to approximately 0.8 d electron, compensated by $6s6p$ screening, and for the divalent metals the d screening is further reduced by ~0.1–0.4 electrons in the respective cases. As a result, the magnitude of the (negative) d screening for the trivalent metals upon $4f$ addition compares well with the (positive) amount of d screening for the divalent metals upon $4f$ removal. The behavior of the $5d$ screening presented in Fig. 5 indicates a substantial difference in screening between removal and addition of $4f$ electrons which will lead to differing SCLS in the two cases in contradiction to the initial-state model.

In Fig. 6, we collect the full calculations of the $4f$ addition level surface shift for the lanthanide metals, taken with reversed sign, and the $4f$ removal surface shift, with the correct sign. These final-state quantities are compared with the initial-state shift of the d-electron LMTO second-order band center C_d,[57,58,24] with reversed sign, i.e.,

$$\Delta_{\text{initial}} = -(C_d^S - C_d^B), \tag{3}$$

between that of a surface (S) and a bulk (B) atom. In addition, we include in Fig. 6 the surface shift of the band center in the separate final states of the $4f$ addition-state

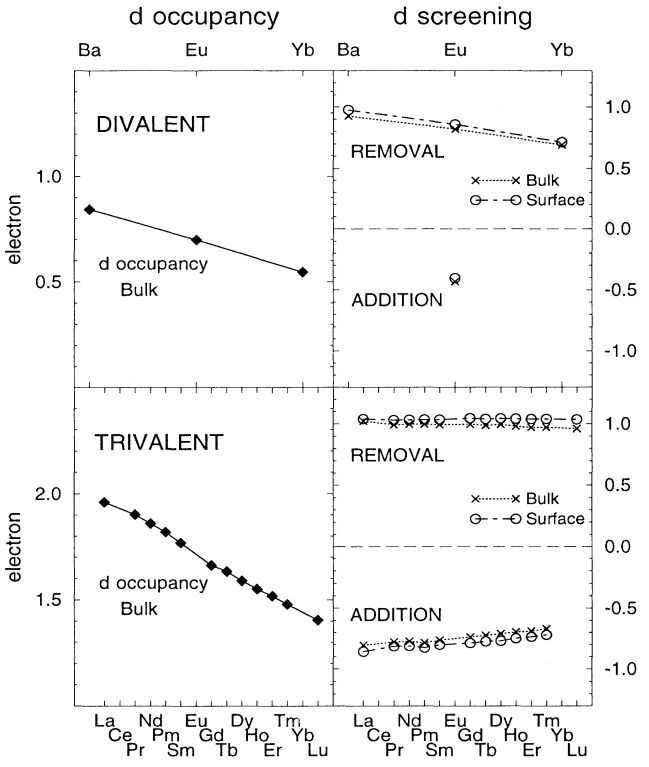

FIG. 5. Left: the calculated valence $5d$ state bulk occupancy of the divalent (top left) and trivalent (down left) rare-earth metals. Right: the calculated $5d$ state contribution to the screening charge on the core-excited impurity atom, defined as the difference in $5d$ state occupancy after and before the $4f$ removal ("REMOVAL") or $4f$ addition ("ADDITION") excitation process.

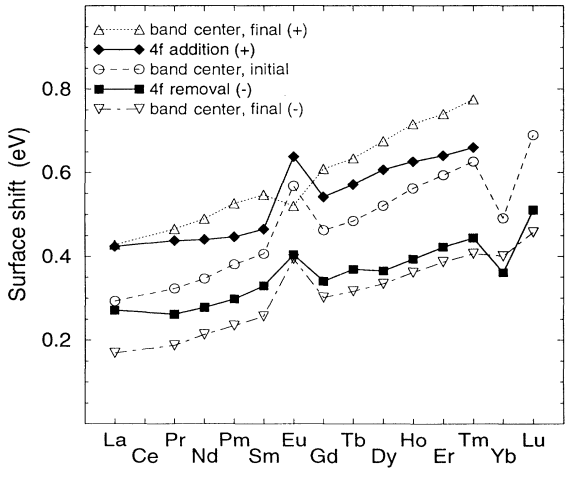

FIG. 6. Comparison between, on the one hand, $4f$ addition surface shifts (solid diamonds) and $4f$-removal surface shifts (solid squares) and, on the other hand, surface shift of the $5d$-state band center referring to the initial state (open circles) and the two different final states of $4f$ addition (open triangles, top curve) and $4f$ removal (open triangles, bottom curve), respectively.

atom and of the $4f$ removal-state atom with the sign convention in accordance with (3). One observes that the bulk to surface shift of the band center falls between the two curves obtained in the final-state calculations.

The behavior of the SCLS in Fig. 6 and the sign convention used in the presentation may be explained by considering a simple model for the screening properties of the d electrons. As shown in Fig. 5, there is for the trivalent lanthanides in the final state essentially an integral increase ($4f$ removal) or decrease ($4f$ addition) in the number of d electrons on the core-ionized impurity atom. Hence the d contribution to the difference in bonding energy between the final and initial states, i.e., the screening energy, may be written

$$E_{\text{screen}}^{\text{one-el}} = \int^{\epsilon_F} (\varepsilon - C_d^{n_d\pm1}) D_d^{n_d\pm1}(\varepsilon) d\varepsilon - \int^{\epsilon_F} (\varepsilon - C_d^{n_d}) D_d^{n_d}(\varepsilon) d\varepsilon, \quad (4)$$

where ϵ_F is the Fermi level, n_d is the number of d electrons in the initial state, and D_d is the local n_d-dependent state density of the d electrons. We then apply a rigid band picture in which the valence states are shifted up (+) or down (−) corresponding to the $4f$ addition or $4f$ removal processes, respectively, by the energy δt whereby $D_d^{n_d\pm1}(\varepsilon)=D_d^{n_d}(\varepsilon\pm\delta t)$. It is convenient to introduce the half-shifted centroid $C_d^{n_d\pm1/2}$, through $C_d^{n_d\pm1}=C_d^{n_d\pm1/2}\mp\delta t/2$ and $C_d^{n_d}=C_d^{n_d\pm1/2}\pm\delta t/2$ and now (4) becomes

$$E_{\text{screen}}^{\text{one-el}} \approx \int^{\epsilon_F\pm\delta t} [\varepsilon \mp \delta t - (C_d^{n_d\pm1/2} \mp \delta t/2)] D_d^{n_d}(\varepsilon) d\varepsilon - \int^{\epsilon_F} [\varepsilon - (C_d^{n_d\pm1/2} \pm \delta t/2)] D_d^{n_d}(\varepsilon) d\varepsilon, \quad (5)$$

which further simplifies into[22]

$$E_{\text{screen}}^{\text{one-el}} \approx \pm(\epsilon_F - C_d^{n_d\pm1/2}). \quad (6)$$

The above one-electron bonding analysis may equally well be applied to the case of surface (S) or bulk (B) screening. Hence if we neglect the impurity aspect and charge transfer, the SCLS may be obtained by the simple estimate

$$\Delta_c \approx \mp(C_d^{S;n_d\pm1/2} - C_d^{B;n_d\pm1/2}), \quad (7)$$

where (−) in front of the paranthesis refers to the $4f$-removal shift and (+) to the $4f$-addition shift, in accordance with the sign convention used in Eq. (2) and in Figs. 3 and 4.

The effect of the difference in screening between the initial and final state is, therefore, approximately accounted for by applying the band-center shift in Eq. (3) for the hypothetical ($n_d \pm 1/2$) intermediate states (cf. Slater's transition state). For the presentation in Fig. 6, however, the band-center shift of the initial ($C_d^{n_d}$) and final ($C_d^{n_d\pm1}$) states are shown together with the full calculations of the $4f$ removal and $4f$ addition shifts, thus decomposing the separate effects of the potential in the initial and final states. Furthermore, only the absolute values are shown, i.e., $-(C_d^{S;n_d} - C_d^{B;n_d})$ and $-(C_d^{S;n_d\pm1} - C_d^{B;n_d\pm1})$, which together with the reversed sign used for the $4f$ addition shift makes the shifts directly comparable with each other.

It is seen in Fig. 6 that the full calculations for the $4f$ removal and $4f$ addition shifts are similarly affected by the initial-state potential, in the sense that the screening takes place in energy levels that are well shifted already in the initial state, and for the trivalent metals this shift increases with increasing atomic number. The surface potential shift relates to the well-known situation for the transition metals where the d-band narrowing in conjunction with an approximate d-charge conservation at the surface produces a shift which scales with the d-band filling. The gradual increase of the potential and band-center shifts across the trivalent lanthanide metals can thus be explained as a combined effect of the reduction of the $5d$ occupancy and the volume contraction which enhances the charge transfer at the surface. In the final state, however, the $5d$ occupancy is either increased or decreased, whereby the band-center shift is significantly larger for the $4f$ addition state than for the $4f$ removal state. This immediately explains the larger magnitudes for the shift of the unoccupied $4f$ level than for the occupied $4f$ level in Fig. 6. In complete agreement with the simplified model the actual surface shifts of the $4f$ states fall between the initial- and final-state band-center shifts. The $4f$-addition shift and the $4f$ removal shift for divalent Eu and Yb, respectively, appear to be an exception, which may partially be attributed to an enhanced impurity effect in these metals and to the reduced influence of the d-electron screening as shown in Fig. 5.

V. CONCLUSION

We have used a Green's-function technique within the tight-binding linear muffin-tin orbitals method to calculate the surface shift of the occupied and unoccupied $4f$ energy positions for the lanthanide metals. In addition, we have calculated the surface energy and work function. Both the occupied and unoccupied $4f$ energy shifts are interpreted within the complete screening picture so as to correspond to the surface segregation energy of a $4f$ ionized impurity in an otherwise unperturbed host. The calculated surface shifts are found to be approximately 0.2–0.3 eV lower in magnitude than the measured data referring to polycrystalline surfaces. In comparison with the single-crystal recordings, however, the agreement between theory and experiment is considerably improved. We find, in agreement with the limited experimental data, that the (negative) surface shift of the unoccupied $4f$ level is approximately 0.2 eV larger in magnitude than the (positive) shift of the occupied $4f$ level. Within a simple one-electron model, this behavior is explained as due to a larger surface shift of the potential in the $4f$ addition final state.

ACKNOWLEDGMENTS

We gratefully acknowledge Professor C. Laubschat and Professor G. Kaindl, and their co-workers in Berlin, for letting us include their data prior to publication. B.J. and M.A. are grateful for financial support from the Swedish Natural Science Research Council. Center for Atomic-Scale Materials Physics is sponsored by the Danish National Research Foundation. Part of this work was supported by grants from the Danish research councils through the Danish Center for Surface Reactivity.

---

* Present address: Max-Planck-Institut für Festkorperforschung, Heisenbergstrasse 1, 70569 Stuttgart, Germany.

[1] G.K. Wertheim and M. Campagna, Chem. Phys. Lett. **47**, 182 (1977).

[2] B. Johansson, in *Rare Earths and Actinides, 1977*, edited by W.D. Corner and B.K. Tanner, IOP Conf. Proc. No. 37 (The Institute of Physics, London, 1978), Chap. 3, p. 39.

[3] G.K. Wertheim and G. Creselius, Phys. Rev. Lett. **40**, 813 (1978).

[4] J.W. Allen, L.I. Johansson, R.S. Bauer, I. Lindau, and S.B.M. Hagström, Phys. Rev. Lett. **41**, 1499 (1978).

[5] B. Johansson, Phys. Rev. B **19**, 6615 (1979).

[6] M. Domcke, C. Laubschat, M. Prietsch, T. Mandel, G. Kaindl, and W.-D. Schneider, Phys. Rev. Lett. **56**, 1287 (1986).

[7] A. Rosengren and B. Johansson, Phys. Rev. B **26**, 3068 (1982).

[8] For a review, see A. Flodström, R. Nyholm, and B. Johansson, in *Advances in Surface and Interface Science, Volume 1: Techniques*, edited by R.Z. Bachrach (Plenum Press, New York, 1992).

[9] J.F. Herbst, D.N. Lowy, and R.E. Watson, Phys. Rev. B **6**, 1913 (1972).

[10] J.F. Herbst, R.E. Watson, and J.W. Wilkins, Phys. Rev. B **17**, 3089 (1978).

[11] F. Gerken, A.S. Flodström, J. Barth, L.I. Johansson, and C. Kunz, Phys. Scr. **32**, 43 (1985).

[12] A.V. Fedorov, C. Laubschat, K. Starke, E. Weschke, K.-U. Barholz, and G. Kaindl, Phys. Rev. Lett. **70**, 1719 (1993).

[13] E. Navas, K. Starke, C. Laubschat, E. Weschke, and G. Kaindl, Phys. Rev. B **48**, 14 753 (1993).

[14] A.V. Fedorov, E. Arenholz, K. Starke, E. Navas, L. Baumgarten, C. Laubschat, and G. Kaindl, Phys. Rev. Lett. **73**, 601 (1994).

[15] G. Kaindl, A. Höhr, E. Weschke, S. Vandré, C. Schüßler-Langeheine, and C. Laubschat (private communication).

[16] A.V. Fedorov, F. Hübinger, and G. Kaindl (unpublished).

[17] C. Laubschat (private communication).

[18] P.J. Feibelman, Phys. Rev. B **39**, 4866 (1989).

[19] M. Methfessel, D. Hennig, and M. Scheffler, Surf. Sci. **287/288**, 785 (1993).

[20] M. Aldén, H.L. Skriver, and B. Johansson, Phys. Rev. Lett. **71**, 2449 (1993).

[21] M. Aldén, H.L. Skriver, and B. Johansson, Phys. Rev. Lett. **71**, 2457 (1993).

[22] M. Aldén, I.A. Abrikosov, B. Johansson, N.M. Rosengaard, and H.L. Skriver, Phys. Rev. B **50**, 5131 (1994).

[23] G. Crecelius, G.K. Wertheim, and D.N.E. Buchanan, Phys. Rev. B **18**, 6519 (1978).

[24] B. Johansson, Phys. Rev. B **20**, 1315 (1979).

[25] B. Johansson and N. Mårtensson, Phys. Rev. B **21**, 4427 (1980).

[26] B. Johansson and N. Mårtensson, Helv. Phys. Acta **56**, 405 (1983).

[27] S.H. Vosko, L. Wilk, and M. Nusair, Can. J. Phys. **58**, 1200 (1980).

[28] O.K. Andersen and O. Jepsen, Phys. Rev. Lett. **53**, 2571 (1984).

[29] O.K. Andersen, Z. Pawlowska, and O. Jepsen, Phys. Rev. B **34**, 5253 (1986).

[30] H.L. Skriver and N.M. Rosengaard, Phys. Rev. B **43**, 9538 (1991).

[31] H.L. Skriver and N.M. Rosengaard, Phys. Rev. B **46**, 7157 (1992).

[32] B. Velický and J. Kurdnovský, Surf. Sci. **64**, 411 (1977).

[33] F. Garcia-Moliner and V.R. Velasco, Prog. Surf. Sci. **21**, 93 (1986).

[34] B. Wenzien, J. Kudrnovský, V. Drachal, and M. Sob, J. Phys. Condens. Matter **1**, 9893 (1989).

[35] H.L. Skriver and N.M. Rosengaard, Phys. Rev. B **45**, 9410 (1992).

[36] M. Aldén, S. Mirbt, H.L. Skriver, N.M. Rosengaard, and B. Johansson, Phys. Rev. B **46**, 6303 (1992); M. Aldén, H.L. Skriver, S. Mirbt, and B. Johansson, Phys. Rev. Lett. **69**, 2296 (1992); Surf. Sci. **315**, 157 (1994).

[37] S. Mirbt, H.L. Skriver, M. Aldén, and B. Johansson, Solid State Commun. **88**, 331 (1993).

[38] N.M. Rosengaard and H.L. Skriver, Phys. Rev. B **47**, 12 865 (1993).

[39] M. Aldén, H.L. Skriver, and B. Johansson, Phys. Rev. B **50**, 12 118 (1994).

[40] F.R. de Boer, R. Boom, W.C.M. Mattens, A.R. Miedema, and A.K. Niessen, in *Cohesion in Metals*, edited by F.R. de Boer and D.G. Pettifor (North-Holland, Amsterdam, 1988), Vol. I, p. 676.

[41] M. Methfessel, D. Hennig, and M. Scheffler, Phys. Rev. B **46**, 4816 (1992).

[42] L. Vitos, J. Kollár, and H.L. Skriver, Phys. Rev. B **49**, 16 694 (1994).

[43] J. Kollár, L. Vitos, and H.L. Skriver, Phys. Rev. B **49**, 11 288 (1994).

[44] O. Gunnarsson, O. Jepsen, and O.K. Andersen, Phys. Rev. B **27**, 7144 (1983).

[45] H.L. Skriver, in *Systematics and the Properties of the Lanthanides*, edited by S.P. Sinha (Reidel, Dordrecht, 1983) p. 239.

[46] H.L. Skriver, Phys. Rev. B **31**, 1909 (1985).

[47] J. Friedel, Ann. Phys. (Paris) **1**, 257 (1976).

[48] For a recent review, see B. Johansson and M.S.S. Brooks, in *Handbook on the Physics and Chemistry of Rare Earths*, edited by K.A. Gschneidner, L. Eyring, G.H. Lander, and G.R. Choppin (North-Holland, Amsterdam, 1993), Vol. 17, p. 149.

[49] H.B. Michaelson, J. Appl. Phys. **48**, 4729 (1977).

[50] A.M. Begley, R.G. Jordan, W.M. Temmerman, and P.I. Durham, Phys. Rev. B **41**, 11 780 (1990).

[51] A.V. Fedorov, A. Höhr, E. Weschke, K. Starke, V.K. Adamchuk, and G. Kaindl, Phys. Rev. B **49**, 5117 (1994).

[52] The calculation for Lu reported in Ref. 22 was performed using the ASA energy functional, and comparison with Table II shows that the presently advocated SCM functional reduces the lowering of the SCLS when proceeding from hcp(0001) to fcc(100). Still, the Lu SCLS for fcc(100) remains surprisingly low.
[53] K. Jacobi, C. Astaldi, B. Frick, and P. Geng, Phys. Rev. B **36**, 3079 (1987).
[54] J.K. Lang, Y. Baer, and P.A. Cox, Phys. Rev. Lett. **42**, 74 (1979).
[55] W.F. Egelhoff, Surf. Sci. Rep. **6**, 253 (1987).
[56] M. Aldén, H.L. Skriver, I.A. Abrikosov, and B. Johansson, Phys. Rev. B **51**, 1981 (1995).
[57] O.K. Andersen, Phys. Rev. B **12**, 3060 (1975).
[58] H.L. Skriver, *The LMTO Method* (Springer-Verlag, Berlin, 1984).
[59] N. Mårtensson, A. Stenborg, D. Björneholm, A. Nilsson, and J.N. Andersen, Phys. Rev. Lett. **60**, 1731 (1988).
[60] A. Stenborg, Ph.D. thesis, Uppsala University, 1989.